TuijinJishu/Journal of Propulsion Technology
ISSN: 1001-4055
Vol. 45 No. 1 (2024)

Investigation of Tensile, Hardness and Double Shear Behaviour of Basalt Aluminium Composites

Sriram K[1*], Bharath Srinivas S [2], VijayaRamanth B [3], Manimaran T[4], Parakh Chandra Mirdul[5], Surendhar S[6]

[1, 2, 3, 4, 5, 6]*Department of Mechanical Engineering, Sri Sai Ram Engineering College, West Tambaram, Chennai, Tamil Nadu, India*

Abstract:-This paper delves into the empirical investigation of a composite laminate comprising Basalt fiber and Aluminum. Basalt, an igneous rock primarily characterized by plagioclase and pyroxene mineral constituents, exhibits significantly enhanced mechanical properties when amalgamated with Aluminum, a soft, non-magnetic, and ductile metal belonging to the boron group. The composite laminate is fabricated employing the hand lay-up method, with the addition of silicon carbide to augment its abrasion resistance and durability. The Basalt-Aluminum laminate is subjected to rigorous testing, encompassing assessments of its ultimate tensile strength via tensile tests, ultimate breaking load, and ultimate stress using double shear tests. Furthermore, the material's hardness is quantified employing the Shore D hardness test. The findings conclusively demonstrate that the inclusion of silicon carbide leads to an augmentation in the ultimate tensile strength and ultimate stress, while simultaneously resulting in a reduction in material hardness. This innovative material exhibits significant promise for deployment in applications where wear and friction are recurrent issues, such as brake calipers, clutch plates, and conveyor belts.

Keywords*: Basalt fiber, Aluminum. Basalt, fiber metal laminates (FML), dynamic mechanical analysis (DMA), silicon carbide (SiC), of abrasive water jet machining (AWJM).*

1. Introduction

In contemporary engineering, the quest for alternative materials to supplant established ones, such as mild steel and cast iron, remains a formidable challenge. These conventional materials, renowned for their commendable mechanical attributes, continue to feature prominently in diverse engineering domains. The exploration of natural fibers, which harbor the potential to rival the properties of incumbent materials, offers a prospective avenue for mitigating the perplexities and quandaries confronting engineers. The amalgamation of Basalt fibers, sourced from volcanic eruptions, represents an economically efficient strategy, synergized with Aluminum, a comparably malleable metal, to engender composite structures capable of manifesting formidable mechanical prowess.

This scholarly exposition embarks upon a comprehensive inquiry into the hand lay-up procedure employed in fabricating fiber metal laminates (FML). It intricately delves into experimental investigations of the shockwave response of fiber metal laminates, particularly scrutinizing gradient aluminum honeycomb sandwich panels as the skin component of the FML structure. The research brings forth critical insights, revealing that the adoption of honeycombs with extended cell side lengths and thickness as the initial layer can induce localized failures within the sandwich panels, thereby influencing their performance [1].

Intricate methods encompassing hand-laid processing techniques are invoked to fuse glass fabric/epoxy laminated composites with matrix reinforcement, incorporating pre-dried graphene nanoplatelets (GNPs) at varying weight percentages, up to 30 wt%. Two discernible categories of E-glass fabrics are deployed in the composite preparation. The investigative arsenal incorporates scanning electron microscopy to facilitate microstructural analysis, uncovering compelling correlations between the number of GNPs introduced and consequential fracture dynamics [2].

The scholarly discourse expounds upon the formidable influence of hand layup compression molding processes, which, in turn, fortify the tensile, flexural, and impact attributes of the material. This fortified material emerges as a viable candidate for application within the commercial automobile sector, resonating with utility in components such as floorings, frames, and bonnets, owing to its hybrid sandwich structure [3][23]. It is pivotal to note that the material under consideration here entails Basalt fiber-reinforced polymer (BFRP) composites, characterized by an epoxy matrix and an intricate assembly of 20 layers, featuring a fiber volume fraction (Vf) of 53.66%. The material's viscoelastic properties are systematically explored across diverse temperature ranges and frequency spectra via dynamic mechanical analysis (DMA), leveraging Basalt fabric constructed in a 2/2 weave pattern [4].

The discourse elegantly elucidates the phenomena of thermal cycling, elucidating how elevations in temperature impart greater ductility to adhesives, causing concomitant reductions in Young's modulus and tensile strength, while simultaneously engendering elevated tensile strain. Inversely, the lowering of temperature precipitates BFRP damage, characterized by delamination and fiber breakage, with the potential for complete delamination failures escalating under these conditions [5].

The authors cogently argue that lightweight fiber-reinforced plastics enjoy primacy within engineering circles, primarily owing to their superior strength-to-weight ratios when juxtaposed with conventional metallic counterparts. It is imperative to discern that fibers, despite their salient advantages, may harbor certain inherent limitations necessitating meticulous consideration for successful amalgamation with metallic substrates. This amalgamation predominantly seeks to harness the strengths of carbon fiber while mitigating its weaknesses, thereby upholding weight efficiency [6].

Within this erudite inquiry, simulated and mechanically characterized Kevlar epoxy-reinforced composites with silicon carbide (SiC) filler are subjected to scrupulous scrutiny. The SiC's inclusion within the Kevlar-reinforced polymer matrix is subjected to a mathematical, software-assisted simulation, and the resulting data is judiciously juxtaposed with experimental findings. The systematic examination spans SiC compositions ranging from 2% to 6%, ultimately unveiling remarkable enhancements, including a surge in tensile strength to 298.22 MPa and a flexural strength of 232.39 MPa, borne out of the infusion of 6% weight percentage of SiC within the Kevlar fiber-reinforced epoxy composite [7][24].

Subsequently, the discourse embarks upon an exploration of glass fiber as the material under investigation. This foray centers on the ramifications of thermo-mechanical loading, meticulously scrutinizing interlaminar shear properties, both under the influence of a 150 MPa static load and through extensive thermal cycling experiments. The results illuminate a nuanced landscape, featuring a 3.6% reduction in interlaminar shear strength following 13,786 cycles, and conversely, a 7.1% augmentation in this property after 36,000 cycles of thermal variation [8][21][22].

This scholarly investigation presents compelling findings that substantiate the proposition that the incorporation of natural Basalt fibers into composites markedly augments their tensile strength. The discerning reader will be informed that the average tensile strength of the Basalt fiber material fabricated in this study reached an impressive 4111 MPa. Furthermore, the criticality of formulation optimization surfaces as a fundamental determinant in technological innovation in the realm of Basalt fiber, promising multifaceted applications [9].

The discourse proceeds to chronicle research endeavors targeting Al-Zn-Mg alloys, wherein 5% and 8% Zn contents and 2 wt% Mg are deftly incorporated using a meticulous solidification process. Post-fabrication, samples are methodically extracted and subjected to an array of sophisticated analyses, including optical microscopy, SEM analysis, energy dispersive spectroscopy, and X-ray diffraction. Notably, these alloys exhibit noteworthy enhancements in ultimate tensile strength and Brinell hardness [10].

Contemplating the Shore hardness test, this paper expounds upon the array of factors that demand meticulous consideration during an extensive series of loading and unloading cyclic tests, characterizing the examination of polymeric structures. Moreover, the comprehensive range in which Shore hardness tests are executed is lucidly elucidated, affording valuable insights for future experimentation [11].

The investigation delves into the realm of double shear tests, specifically dissecting their applicability to composite structures comprising fiber-reinforced cementitious matrices. This scholarly undertaking, replete with insightful narratives, catalogs a diverse array of potential outcomes that may arise from the execution of double shear tests, permitting an informed understanding of load distribution within composite structures [12].

The discourse then transitions towards the examination of graphene composites, meticulously reinforcing them with hemp fibers. The efficiency of hemp fiber laminates augmented with NaOH is systematically assessed, culminating in noteworthy enhancements in both flexural and hardness properties, thus rendering them highly suitable for engineering applications [13].

In a holistic view of material choice and the methodologies underpinning composite material reinforcement, the synthesis of glass fiber and natural fibers, in conjunction with the inclusion of polyester resin, is subjected to a scrupulous inquiry via the hand layup method. The material compositions are systematically diversified, culminating in a series of meticulous mechanical and water absorption tests, the results of which are judiciously cataloged for comprehensive analysis [14].

Moving forward, the author embarks upon a detailed discussion of aluminum-3.8Cu-Cr alloys, enriched with 0.25 and 0.5 wt% of chromium additives. The methodology entails a solidification process, followed by microstructural examination of specimens, rigorous hardness assessments, and tensile tests. Notably, these alloys are found to be exceedingly efficacious in augmenting both the Al–3.8Cu–0.50Cr material's properties [15].

Researchers meticulously navigate the intricacies of mechanical experimentation, adroitly harnessing abaca, jute, flax, and kenaf as both mono-fiber and hybrid-fiber composites via the hand layup method. The findings unequivocally demonstrate the superior performance of hybrid composites in contrast to their mono-fiber counterparts [16].

The discussion unfolds to encompass a meticulous analysis of Sn-Pb solder alloys, encompassing varying compositions, with lead (Pb) constituting 15%, 60%, and 80% of the alloy. These alloy configurations are subjected to extensive tensile and hardness testing, subsequent to controlled exposure to temperature ranges spanning 350°C. Astonishingly, the results underscore the enhancement in hardness and tensile properties, especially in the composition featuring 60% Pb-Sn alloy [17].

The paper ultimately navigates into an exploration of natural fibers, including Jute-Flax, Banana-Flax, Abaca-Jute, Banana Jute, and Basalt-Banana composites. Mechanical behaviors of these hybrid composites are scrutinized, revealing the undeniable supremacy of hybrid configurations in terms of mechanical performance, thereby advocating their utility in engineering applications [18], [19].

An investigation with boron carbide and silicon carbide compositions within aluminium alloy 6061composite's shows superiority in tensile, flexural strength, hardness, and impact resistance over pure aluminium. Furthermore, they observed that the microstructural analysis by SEM found few defects in casted composites [25]. It was focused on comprehending the impact of pin profile alterations and rotational speed variations on microstructural attributes and tensile strength, which involved sophisticated adjustments to welding parameters. They utilized advanced microscopy and meticulous tensile strength testing methodologies, this research endeavours to contribute to the reinforcement of dissimilar alloy welding techniques, fostering diverse industrial applications [26]. An optimization work on the process parameters of abrasive water jet machining (AWJM) of nickel alloy. They focused on kerf taper angles through conventional analytical methodologies, with the goal of refining machining precision and operational efficiency. They concluded that endeavour holds promise for elevating the quality and accuracy of nickel alloy machining operations [27]. Composites laminates fortified with abaca fibers, focusing on their potential application within the automotive sector. They found that mechanical behaviour of abaca based laminate is better than mono fibre laminates. [28]

2. Materials and Methods

2.1. Basalt fiber

Within this study, basalt fiber emerges as a pivotal reinforcement material endowed with versatile applicability, extending to areas such as the construction of corrosion-resistant pipelines, the development of non-inflammable coverings, and the production of high-performance components like brake calipers and clutch plates. Basalt fiber, an igneous rock derivative, originates from the expeditious solidification of molten volcanic material upon its exposure to the Earth's surface. These basalt fibers manifest in diverse formats, encompassing chopped fabric, rolls, and powdered iterations, facilitating a broad spectrum of engineering possibilities.

2.2. Aluminium

Aluminum, a lustrous, silvery-white element, is a lightweight and highly malleable metallic alloy. Remarkably, it ranks among the most plentiful elements within the Earth's crust. The composite material in question is meticulously engineered utilizing a mesh derived from the 5000 series of aluminum alloy.

2.3. Epoxy Resin

In this endeavor, the epoxy composite under investigation employs Araldite LY 556 as the epoxy resin component, a formulation primarily predicated on Bisphenol-A, coupled with the deployment of Aradur HY 951 as the hardening agent. This resin system demonstrates remarkable superiority in terms of flexural strength, adhesive properties, and fatigue resistance.

The experimental composition features Araldite LY 556, an epoxy resin that finds its foundation in the molecular architecture of Bisphenol-A and is adeptly conjoined with the precise incorporation of Aradur HY 951 as the reactive hardening agent. Notably, the resultant composite manifests an exceptional degree of excellence, particularly with regard to its flexural strength, adhesive characteristics, and fatigue resistance.

The investigation at hand delves into the utilization of the epoxy matrix, Araldite LY 556, which is intricately based on the Bisphenol-A framework, and is skillfully augmented by the introduction of Aradur HY 951 as the hardening agent. The ensuing composite material exhibits a notable and distinguished degree of superiority, particularly in terms of its flexural strength, adhesive attributes, and remarkable resilience against the deleterious effects of fatigue.

2.4. Silicon Carbide

Silicon carbide is a semiconducting compound comprising silicon and carbon, characterized by its inherently high hardness and exceptional resistance to wear. It possesses remarkable qualities, including outstanding chemical and thermal shock resistance. This material finds extensive utility in diverse applications, such as diodes, MOSFETs, brake pads, grinding wheels, clutch plates, and even in the manufacturing of bulletproof vests.

2.5. Methodology

The composite material is meticulously crafted through the utilization of epoxy resin, incorporating silicon carbide (SiC) in varying weight percentages of 3% and 6%. This intricate fabrication process employs the meticulous hand layup method, followed by precision compression molding techniques.

2.6. Hand layup Method

This methodology represents a facile and straightforward approach to fabricating natural fiber composites. While the fabrication process is characterized by a notably leisurely pace, it remains universally applicable to a wide array of fiber types. In the context of this research, the layup procedure entails a meticulous arrangement of individual basalt fiber plies by manual stacking, with subsequent precision placement of aluminum layers atop successive strata of basalt. Within this composite assembly, an epoxy resin is judiciously combined with silicon carbide (SiC) to serve as an interstitial adhesive substance, imparting cohesiveness between the basalt and aluminum strata. The consolidation of the composite structure is meticulously achieved through the utilization of a compression molding process, thereby obviating the presence of undesirable air pockets between the strata.

3. Testing of composites

3.1. Tensile Test

The tensile testing procedure typically involves employing specimens with a centrally located region of uniform cross-sectional dimensions. This specific region, known as the gauge length, may possess either uniform circular or rectangular geometry. The broader extremities of the specimen are affixed to the grips of a universal testing machine, and these broader regions are referred to as the gripping ends. The preparation of specimens conforms to the prescribed standards, such as ASTM D638, as depicted in Figure 1. The initial state of a specimen prior to undergoing tensile testing is illustrated in Figure 2.

The specimens are meticulously mounted onto the universal testing machine, and loads are incrementally applied with precision to accurately ascertain the material's strength. During the operation of the universal testing machine, an exerted force acts upon the specimen, aiming to elongate and separate it. This force, responsible for stretching the specimen, is termed the tensile force.

In the course of subjecting the specimen to this tensile force, an alteration occurs in its original length, manifesting as an instantaneous length, indicative of a measurable elongation relative to the initial length. At a distinct juncture, a marked departure from linear deformation is observed, leading to necking—a localized constriction—in the structural integrity of the specimen. This notable transformation in the cross-sectional area of the specimen is observed as it approaches the ultimate tensile stress of the material, culminating in the formation of a necking feature on the specimen's surface, as depicted in Figure 3.

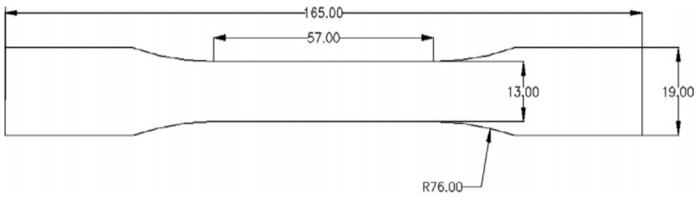

Figure. 1 Tensile Test specimen - ASTM D638

Figure. 2 Specimen Before Tensile Test

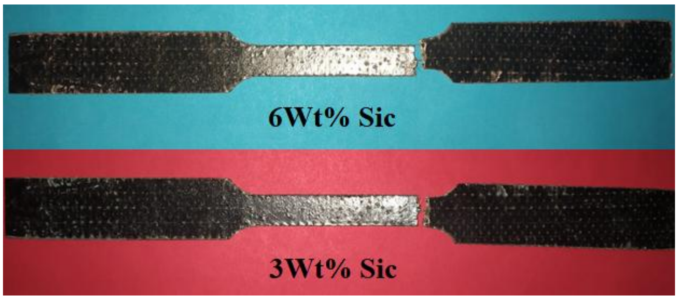

Figure. 3 Specimen After Tensile Test

3.2. Double Shear Test

The universal testing machine serves as a versatile instrument for conducting a spectrum of mechanical assessments, encompassing tensile, compression, and torsional tests. In this context, specimens containing 3 and

6wt% SiC are meticulously tailored to conform to the requisite dimensions stipulated by the established testing laboratory standards, as vividly delineated in Fig. 4.

The specimen is impeccably positioned within the double shear dies, and subsequently, it is affixed to one extremity of the upper attachment through the agency of a gripper. Thereafter, the other end is similarly secured at the lower terminus. The dies, housing the specimen earmarked for experimentation, are introduced onto the universal testing machine, and the entire apparatus is diligently configured to ensure precision.

Progressively incrementing loads are applied to the specimen. At a specific juncture, discernible shear forces manifest within the specimen. The precise load at which shear becomes evident is meticulously recorded, as depicted in Fig. 5. Subsequently, Fig. 5 illustrates the specimen's configuration post-testing, revealing that it has been partitioned into three distinct segments for both the 3 and 6 wt% SiC specimens, respectively.

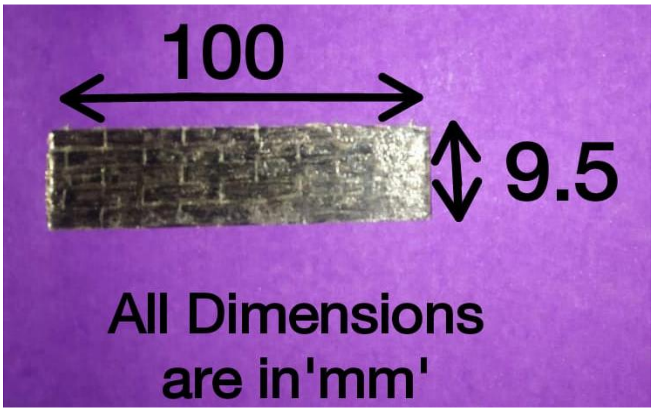

Figure. 4 Specimen Before Double Shear Test

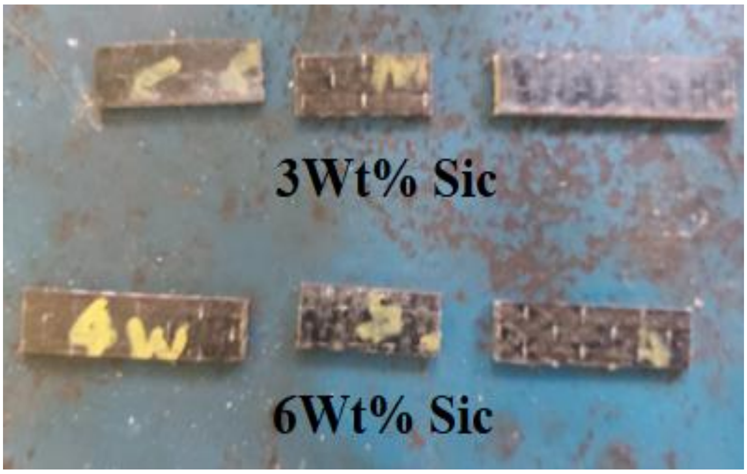

Figure. 5 3 and 6 wt% SiC Specimen After Double Shear Test

3.3. Shore D Hardness Test

Materials possessing inherent low rigidity, such as supple rubbers, polymers, and plastics, present an impractical challenge for conventional hardness evaluation methods like Rockwell or Brinell hardness tests. Instead, these materials necessitate the employment of a distinct hardness assessment technique recognized as Shore D Hardness, specifically designed to gauge the material's resistance to the intrusion of a stylus with a blunted tip, simulating a spring-like characteristic. The apparatus instrumental in executing this examination is referred to as a "durometer." Shore Hardness is categorized into two primary types, namely "A-type hardness" and "D-type hardness." The former is applied when characterizing the softest elastomers, employing a blunted-point stylus, whereas the latter, Shore D hardness, is utilized when assessing the hardness of more rigid elastomeric materials. In the case of Shore D hardness, a stylus inclined at a 30-degree angle is employed for the test.

The procedure for hardness testing necessitates meticulous adherence to the ASTM D2240 standard to ensure consistent and standardized results. An illustrative representation of the specimen is presented in Figure 6. This specimen is positioned atop an adjustable platform. Prior to commencing the hardness examination, the durometer must undergo meticulous calibration and scrutiny to mitigate any deviations that may potentially influence measurement accuracy.

The specimen is then positioned on the platform, and the durometer is meticulously lowered onto the surface of the specimen, as depicted in Figure 7. The application of force via the durometer stylus must be executed uniformly and methodically, with utmost precision to prevent inadvertent aberrations or surface disturbances during the testing process.

Figure. 6 Shore D Hardness Test Specimen

Figure. 7 Shore D Hardness Test

4. Result and Discussion

4.1. Result of tensile Test

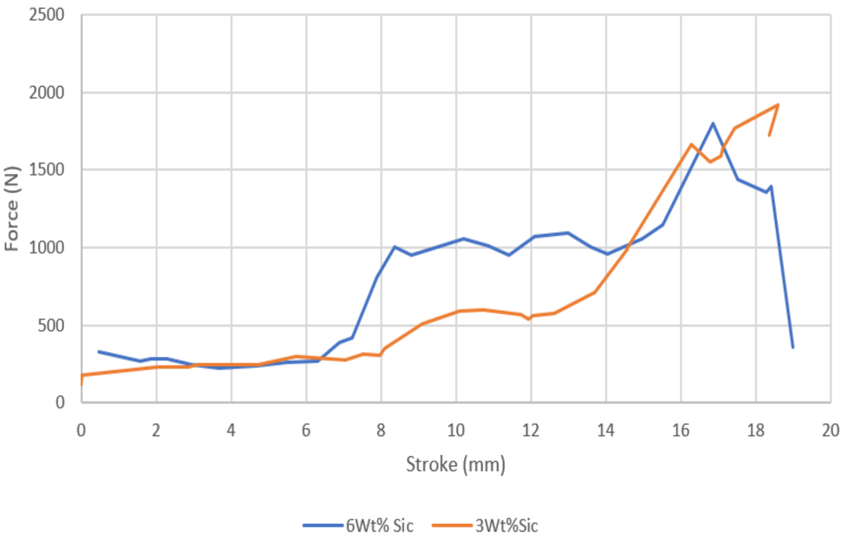

Figure. 8 Force vs Stroke Graph for 6and3wt% SiC Specimen

Table 1. Tensile Test Results

Specimen	Fmax (N)	Ultimate Tensile Strength (Mpa)
6wt% SiC	1,800	55.94
3wt% SiC	1,980	64.82
Difference	180	8.88
Percentage	110.0%	115.87%

The graphical representations in Figure 8 have been subjected to comprehensive analysis, and the pertinent data has been meticulously tabulated, as delineated in Table 1. Upon scrutiny, it becomes evident that the specimen incorporating 6 weight percent (wt%) of silicon carbide (SiC) exhibits a Tensile Strength of 55.94 megapascals (MPa) and attains an Fmax of 1,800 newtons (N). In contrast, the composite containing 3 wt% SiC manifests a Tensile Strength of 64.82 MPa and achieves an Fmax of 1,980 N.

The aforementioned outcomes lead to a compelling conclusion: the composite specimen featuring 3 wt% SiC surpasses its counterpart with 6 wt% SiC, demonstrating superior Tensile Strength by 8.88 MPa and an elevated Fmax of 180 N. This noteworthy difference corresponds to an enhancement of 1.1 and 1.158 times, respectively, when directly juxtaposed with the performance of the 6 wt% SiC specimen.

4.2. Result of double Shear Test

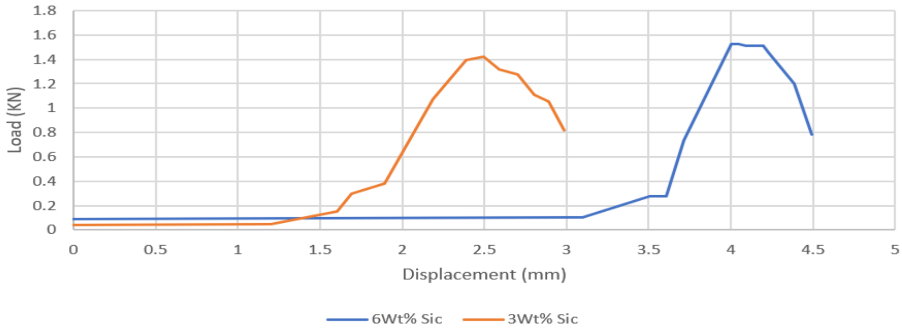

Figure. 9 Load vs Displacement Graph of 3 and 6 wt% SiC Specimen

Table 2. Double Shear Test Results

Specimen	Ultimate Break Load (N)	Ultimate Stress (N/mm^2)
6wt% SiC	1,525	136
3wt% SiC	1,415	126
Difference	110	10
Percentage	107.77%	107.93%

The graphical data in Figure 9 has been subjected to meticulous analysis, and the findings have been meticulously organized in Table 2. It has been discerned that the specimen comprising 3 weight percent (wt%) of silicon carbide (SiC) exhibits an ultimate breaking load of 1,415 Newtons (N) and an ultimate stress of 126 N/mm^2. Conversely, the specimen containing 6 wt% SiC demonstrates superior performance, boasting an ultimate breaking load of 1,525 N and an ultimate stress of 136 N/mm^2.

The foregoing results establish a decisive superiority of the composite specimen with 6 wt% SiC over its counterpart with 3 wt% SiC. Notably, the former exhibits an impressive increase of 110 N in ultimate breaking load and a substantial enhancement of 10 N/mm^2 in ultimate stress, equating to an improvement of approximately 1.077 and 1.079 times, respectively, when juxtaposed with the 3 wt% SiC specimen.

4.3. Result of HardnessTest

Table 3. Shore D Hardness Test Results

Specimen	Trial 1	Trial 2	Trial 3	Average	Average - High	Average - Low
6wt% SiC	67	67.5	64.2	66.233	-1.267	2.0333
3wt% SiC	73.7	73.7	63.3	70.233	-3.467	6.9333

The recorded data has been meticulously tabulated, as depicted in Table 3. Upon analysis, it has been ascertained that the composite specimen infused with 6wt% SiC exhibits an average hardness of 66.233, with hardness values falling within the range of 64.966 to 68.266. Conversely, the composite sample containing 3wt% SiC demonstrates an average hardness of 70.233, with individual hardness values spanning from 66.773 to 77.166.

This empirical outcome leads to the unequivocal conclusion that the composite specimen with 3wt% SiC surpasses its counterpart containing 6wt% SiC in terms of hardness by a margin of 4 units. This remarkable improvement represents a 1.060-fold increase in hardness when directly compared to the composite specimen with 6 wt% SiC.

5. Conclusion

The Tensile strength tests yielded values of 55.94 MPa and 64.82 MPa for the ultimate tensile strength, pertaining to SiC content levels of 6wt% and 3wt%, respectively. It is worth noting that the tensile strength exhibited by this composite of aluminum and basalt is on par with that of unreinforced polyester resin and ultra-high molecular weight polyethylene, signifying a notable mechanical equivalence. The introduction of SiC into the aluminum-basalt composite is conclusively demonstrated to bolster its tensile strength.

Furthermore, an assessment of double shear test results indicates that the inclusion of SiC leads to a remarkable 7.77% augmentation in the ultimate stress of the laminate. This enhancement underscores the beneficial impact of SiC as an augmentation agent in enhancing the composite's mechanical properties.

In the context of the Shore D hardness test, it is discerned that the material's hardness aligns favorably with that of a hard hat. It is noteworthy that the incorporation of SiC appears to engender a decrease in the composite material's hardness, thereby imbuing it with heightened flexibility, a pivotal attribute in various engineering applications.

References

[1] X. Ma, X. Li, S. Li, R. Li, Z. Wang, and G. Wu, “Blast response of gradient honeycomb sandwich panels with basalt fiber metal laminates as skins,” International Journal of Impact Engineering, vol. 123, pp. 126–139, Jan. 2019, doi: 10.1016/j.ijimpeng.2018.10.003.

[2] G. v. Seretis, G. Kouzilos, D. E. Manolakos, and C. G. Provatidis, “On the graphene nanoplatelets reinforcement of hand lay-up glass fabric/epoxy laminated composites,” Composites Part B: Engineering, vol. 118, pp. 26–32, Jun. 2017, doi: 10.1016/j.compositesb.2017.03.015.

[3] M. S. Santhosh et al., “Fabrication and Characterization of Basalt/Kevlar/Aluminium Fiber Metal Laminates for Automobile Applications,” 2019. [Online]. Available: http://www.ripublication.com

[4] K. Karvanis, S. Rusnáková, O. Krejčí, and M. Žaludek, “Preparation, thermal analysis, and mechanical properties of basalt fiber/epoxy composites,” Polymers, vol. 12, no. 8, Aug. 2020, doi: 10.3390/polym12081785.

[5] J. Na, W. Mu, G. Qin, W. Tan, and L. Pu, “Effect of temperature on the mechanical properties of adhesively bonded basalt FRP-aluminum alloy joints in the automotive industry,” International Journal of Adhesion and Adhesives, vol. 85, pp. 138–148, Oct. 2018, doi: 10.1016/j.ijadhadh.2018.05.027.

[6] C. Hühne, C. Hühne, and E. Petersen, “Fiber-Metal-Laminates Elliptical Biaxial Fatigue Testing of Wind Energy Rotor Blades View Project Composites mechanical properties characterisation View project FIBER-METAL-LAMINATES,” 2014. [Online]. Available: https://www.researchgate.net/publication/312169586

[7] A. Suresh, P. Bhargavi, and M. Kiran Kumar, “Simulation and mechanical characterization on Kevlar epoxy reinforced composite with silicon carbide filler,” in Materials Today: Proceedings, 2020, vol. 38, pp. 2988–2995. doi: 10.1016/j.matpr.2020.09.321.

[8] M. Hagenbeek and J. Sinke, “Effect of thermal cycling heated Fibre Metal Laminates under static load,” Composite Structures, vol. 211, pp. 540–545, Mar. 2019, doi: 10.1016/j.compstruct.2018.12.042.

[9] Y. Meng, J. Liu, Y. Xia, W. Liang, Q. Ran, and Z. Xie, “Preparation and characterization of continuous basalt fibre with high tensile strength,” Ceramics International, vol. 47, no. 9, pp. 12410–12415, May 2021, doi: 10.1016/j.ceramint.2021.01.097.

[10] B. P. Reis, M. M. Lopes, A. Garcia, and C. A. dos Santos, “The correlation of microstructure features, dry sliding wear behavior, hardness and tensile properties of Al-2wt%Mg-Zn alloys,” Journal of Alloys and Compounds, vol. 764, pp. 267–278, Oct. 2018, doi: 10.1016/j.jallcom.2018.06.075.

[11] Z. Liao, M. Hossain, and X. Yao, “Ecoflex polymer of different Shore hardnesses: Experimental investigations and constitutive modelling,” Mechanics of Materials, vol. 144, May 2020, doi: 10.1016/j.mechmat.2020.103366.

[12] L. H. Sneed, T. D’Antino, C. Carloni, and C. Pellegrino, “A comparison of the bond behavior of PBO-FRCM composites determined by double-lap and single-lap shear tests,” Cement and Concrete Composites, vol. 64, pp. 37–48, Nov. 2015, doi: 10.1016/j.cemconcomp.2015.07.007.

[13] B. VijayaRamnath, S. Gowtham, J. Melvin Antony, D. Kumaran, and G. Lokeshwaran, “Investigations of Flexural and Hardness Behaviour of Graphene Composites,” in IOP Conference Series: Materials Science and Engineering, Oct. 2020, vol. 954, no. 1. doi: 10.1088/1757-899X/954/1/012004.

[14] C. M. Meenakshi and A. Krishnamoorthy, “Preparation and mechanical characterization of flax and glass fiber reinforced polyester hybrid composite laminate by hand lay-up method,” 2018. [Online]. Available: www.sciencedirect.comwww.materialstoday.com/proceedings2214-7853

[15] T. M. Ribeiro, E. Catellan, A. Garcia, and C. A. dos Santos, “The effects of Cr addition on microstructure, hardness and tensile properties of as-cast Al-3.8wt.%Cu-(Cr) alloys,” Journal of Materials Research and Technology, vol. 9, no. 3, pp. 6620–6631, 2020, doi: 10.1016/j.jmrt.2020.04.054.

[16] B. VijayaRamnath, S. JunaidKokan, R. Niranjan Raja, R. Sathyanarayanan, C. Elanchezhian, A. Rajendra Prasad, and V. M. Manickavasagam. “Evaluation of mechanical properties of abaca–jute–glass fibre reinforced epoxy composite,” Materials & Design 51 (2013): 357-366.

---

[17] O. R. Adetunji, R. A. Ashimolowo, P. O. Aiyedun, O. M. Adeusi, H. O. Adeyemi, and O. R. Oloyede, "Tensile, hardness and microstructural properties of Sn-Pb solder alloys," in Materials Today: Proceedings, 2021, vol. 44, pp. 321–325. doi: 10.1016/j.matpr.2020.09.656.

[18] Sakthivel, M., S. Vijayakumar, and B. VijayaRamnath. "Investigation on mechanical and thermal properties of stainless-steel wire mesh-glass fibre reinforced polymer composite," Silicon 10.6 (2018): 2643-2651.

[19] G. Ramakrishnan, B. VijayaRamnath, C. Elanchezhian, A. Arun Kumar, and S. Gowtham. "Investigation of mechanical behaviour of basalt-banana hybrid composites," Silicon 11, no. 4 (2019): 1939-1948.

[20] VR Raman Bharath, B VijayaRamnath, N Manoharan, Kenaf fibre reinforced composites: a review, ARPN J. Eng. Appl. Sci 10, 5483-5485.

[21] BV Ramnath, J Jeykrishnan, G Ramakrishnan, Sea shells and natural fibres composites: a review , Materials Today: Proceedings 5 (1), 1846-1851.

[22] P Kaliappan, R Kesavan, B VijayaRamnath, Investigation on effect of fibre hybridization and orientation on mechanical behaviour of natural fibre epoxy composite, Bulletin of Materials Science 40 (4), 773-782

[23] S Rajesh, BV Ramnath, C Elanchezhian, M Abhijith, RD Riju, KK Kishan,, Investigation of tensile behavior of Kevlar composite, Materials Today: Proceedings 5 (1), 1156-1161

[24] A Abinash , BV Ramnath, , B Srinivasan, RV Nair, , Investigation of mechanical behaviour of sisal epoxy hybrid composites, Indian Journal of Science and Technology 9, 34.

[25] P Subramanya Reddy, R Kesavan, B VijayaRamnath , Investigation of mechanical properties of aluminium 6061-silicon carbide, boron carbide metal matrix composite., Silicon 10: 495–502,2018.

[26] K Palani, C Elanchezhian, BV Ramnath, GB Bhaskar, E Naveen , 'Effect of pin profile and rotational speed on microstructure and tensile strength of dissimilar AA8011, AA01-T6 friction stir welded aluminum alloys", Materials Today: Proceedings 5 (11), 24515-24524, 2018.

[27] J Jeykrishnan, BV Ramnath, SS Vignesh, P Sridharan, B Saravanan, "Optimization of process parameters in abrasive water jet machining/cutting (AWJM) of nickel alloy using traditional analysis to minimize kerf taper angle Materials Today: Proceedings 16, 392-397, 2019.

[28] V.M. Manickavasagam, "Fabrication and testing of abaca fibre reinforced epoxy composites for automotive applications", Advanced Measurement and Test III, 63, 2013.